HEAT EXCHANGERS

Energy Conversion Technical Report No. 10

by

B. P. EDWARDS

June 1975

Department of Engineering Physics
Research School of Physical Sciences
THE AUSTRALIAN NATIONAL UNIVERSITY
Canberra, A. C. T. Australia.

HEAT EXCHANGERS

Energy Conversion Technical Report No. 10

by

B. P. EDWARDS

June 1975

Department of Engineering Physics
Research School of Physical Sciences
THE AUSTRALIAN NATIONAL UNIVERSITY
Canberra A. C. T. Australia

CONTENTS

INTRODUCTION

The need for counterflow heat exchangers in the ANU design of a large scale solar plant has already been described.[1] The components of this system are shown schematically in Figure 1. The heat exchangers involved will be required to heat or cool either ammonia or a mixture of nitrogen and hydrogen gases over the range from ambient to 700°C, at pressures around 300 atmospheres. Over this range species properties vary considerably and digital techniques are necessary in a domain where standard formulae are inapplicable due to this variation. The present report describes a numerical study of the performance of the heat exchanger design, which enabled accurate estimates of the size of the heat exchanger required. The report does not contain a theoretical basis for the heat exchanger configuration, as this was primarily determined by the difficulties associated with manufacture.

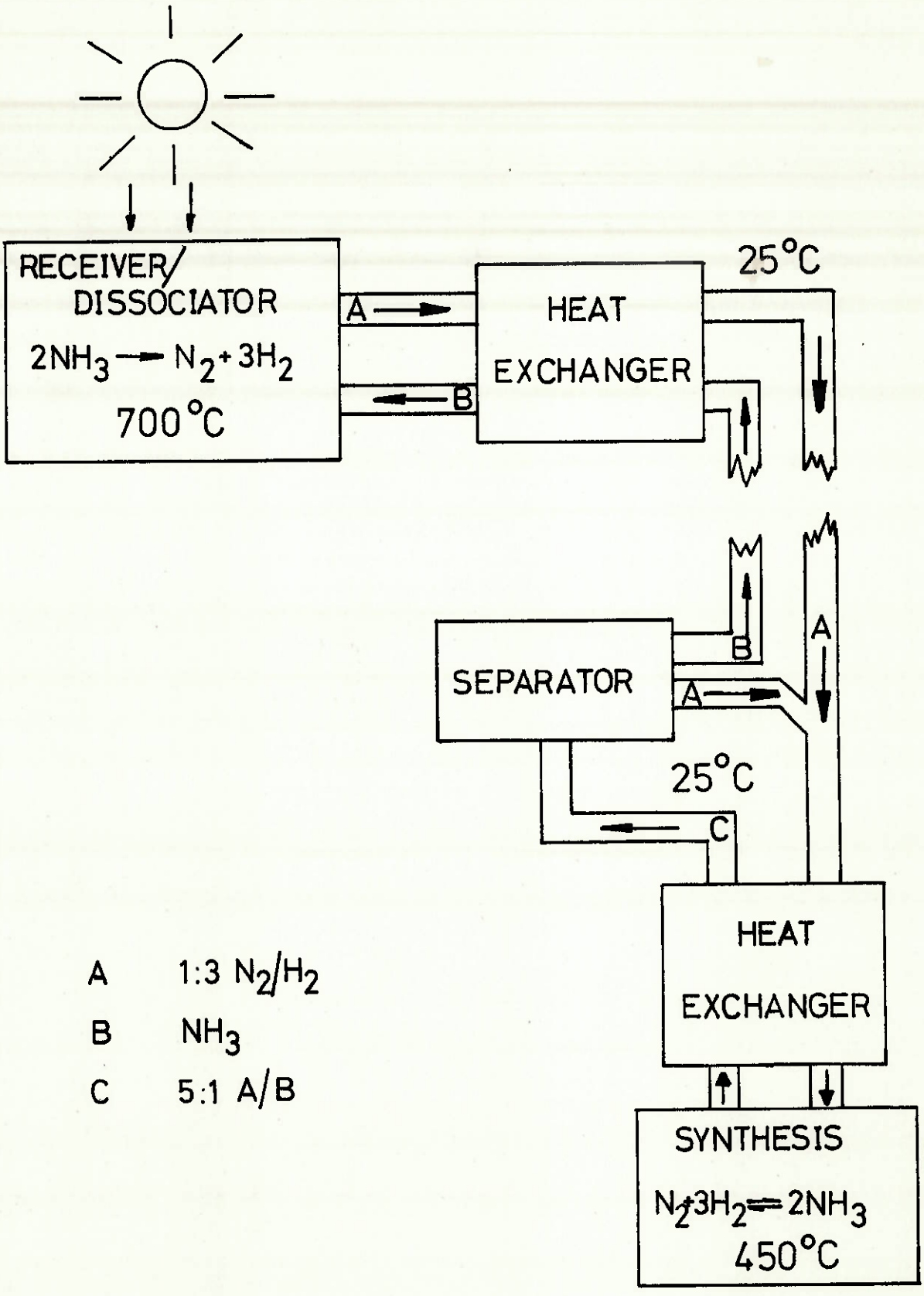

Figure 1. A.N.U. Energy Transport and Recovery System.

2. THEORY OF HEAT EXCHANGERS

A heat exchanger, in essence, consists of two passages, thermally linked by a membrane of conductivity $\bar{U}_1$ (cal/(sec-cm-^{o}C)). Each passage supports a mass flow rate of $\dot{m}$ grams/sec, assumed the same for both sides. The situation considered in the theory is shown in Figure 2.

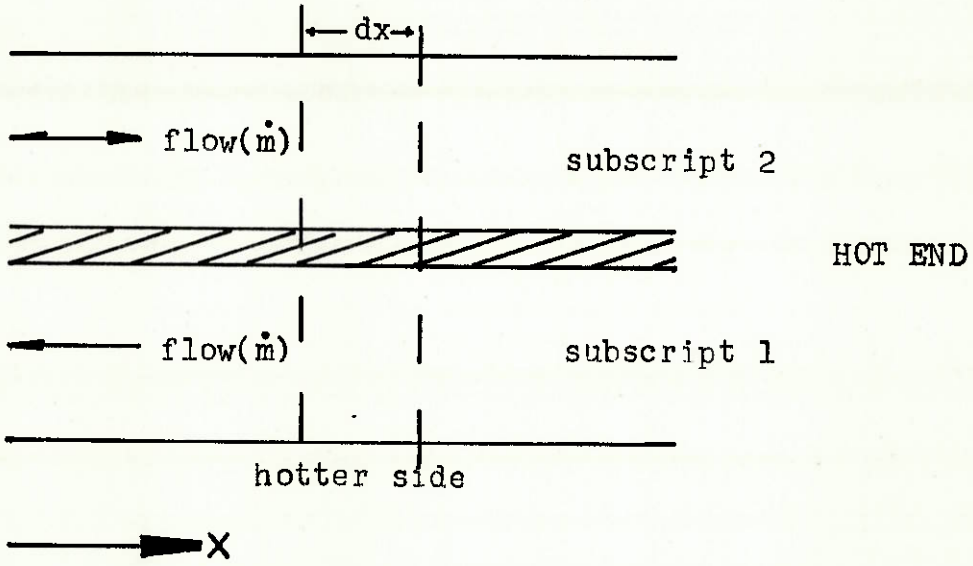

Figure 2.

We can then obtain two equations: -

(A) relating the temperature rise in one side to the heat flow $d\dot{Q}$ (cal/sec)

$$d\dot{Q} = \dot{m}\ c_{p1}\ dT_1 \qquad c_p = \text{specific heat (cal/gm)}$$

(B) relating the heat flow to the temperature difference between the two sides

$$d\dot{Q} = \bar{U}_1\ dx\ (T_1 - T_2)$$

Combining these, we obtain

$$\dot{m}\ c_{p1}\ \frac{dT_1}{dx} = \bar{U}_1\ (T_1 - T_2) \qquad (1)$$

$$\dot{m}\ c_{p2}\ \frac{dT_2}{dx} = \bar{U}_1\ (T_1 - T_2) \qquad (2)$$

Note that over the incremental length dx, these equations hold regardless of the temperature dependence of the specific heat and $\bar{U}_1$.

3. ANALYTICAL SOLUTIONS

By differentiating (2) and substituting in (1) or vice versa, we obtain

$$\frac{d^2T}{dx^2} = \frac{\bar{U}_1}{\dot{m}} \left(\frac{.1}{c_{p1}} - \frac{.1}{c_{p2}}\right) \frac{dT}{dx} \qquad (3)$$

$$\text{let } b = \frac{\bar{U}_1}{\dot{m}} \left(\frac{1}{c_{p1}} - \frac{1}{c_{p2}}\right)$$

$$\text{Then } \frac{d^2T}{dx^2} - b\frac{dT}{dx} = 0$$

Assuming c_p and T are not functions of temperature,

$$T = \frac{1}{b} Ae^{bx} + B$$

By fitting two boundary conditions

$$\text{viz } T = T_h \text{ at } x = L$$

$$T = T_c \text{ at } x = 0$$

we can obtain the constants

$$A = \frac{b(T_h - T_c)}{e^{bL} - 1}$$

$$B = \frac{T_c - T_h e^{-bL}}{1 - e^{-bL}}$$

For engineering calculations, the above assumptions lead to a relation between the total length of the heat exchanger L and the heat transferred per second $\dot{Q}$, viz

$$L = \frac{\dot{Q}}{\bar{U}_1 \Lambda}$$

where Λ is the log mean temperature difference

$$\Lambda = \frac{(T_{h1} - T_{h2}) - (T_{c1} - T_{c2})}{\ln \left(\frac{T_{h1} - T_{h2}}{T_{c1} - T_{c2}}\right)}$$

This standard solution is derived in Zemansky.[2]

The Heat Transfer coefficient $\bar{U}_1$

The conductivity between the two fluids is determined by three factors: the two boundary layers and the metal wall between the two fluids.

a) The metal alloys of chromium, nickel and iron are necessary to withstand the corrosion by the fluids involved, and their thermal conductivity is well documented by the manufacturers.[3]

b) The boundary layers. Zemansky[2] gives the value of the convection coefficient h for a turbulent flow in a pipe of diameter D as:

$$\frac{hD}{k} = 0.023 (Re_D)^{0.8} (P_r)^{0.4}$$

where Re_D is the Reynolds number based on diameter and P_r the Prandtl number.

By the use of a hydraulic radius, and knowledge of the pipe perimeter p, we may use this formula for a square pipe, with

$$\frac{h_1 D}{p\, k} = 0.023 (Re_D)^{0.8} (P_r)^{0.4}$$

where h_1 is the thermal conductivity per unit length.

The conductivity of the metal is given by

$dh_1 = \frac{dp}{x} k$ where x is the path length for heat flow from a section of the perimeter dp. This is not known a priori, however, as the conductivity of metals is usually far higher than the boundary layers, we

take x as the distance between the channels.

$$h_1 = \frac{pk}{x}$$

This problem is approximated more thoroughly later.

The three thermal conductivities/unit length are combined, viz

$$(\bar{U}_1)^{-1} = (h_1\,(NH_3))^{-1} + (h_1\,(\text{metal}))^{-1} + (h_1\,(N_2/3H_2))^{-1}$$

4. THE NEED FOR DIGITAL SOLUTION

Unfortunately the present system does not satisfy either of the two assumptions, viz the ammonia undergoes a phase change between the two ends of the heat exchanger which involves not only variations in specific heat, but also considerable variations in viscosity (a factor of five), which affect the convection coefficient. As well as this, only two temperatures in the system are defined, viz the cold side at the cold end, and the hot side at the hot end. What we wish to determine is the amount of energy loss from the cold end of the exchanger (represented by the temperature difference between the fluids at the cold end), and compromise this with an acceptable length of exchanger. Due to the abovementioned temperature dependence of the quantities involved, one needs to integrate eqns (1) and (2) on page 3 in a stepwise manner.

5. METHOD OF DIGITAL SOLUTION

Several methods exist for integrating a system of equations of the form:

$$y = f(x, y, y_2)$$

and these are well documented by Gear.[4] Serious consideration was given to the Bulirsch-Stoer algorithm, however, the simplicity and time involved in programming a Runge-Kutta method overrode the possible increase in

computational efficiency accorded to the former method. Also the functions involved are well behaved, and the possibility of integration problems seemed remote. Accordingly the two equations were integrated using a fourth order Runge-Kutta method. For the integration routine, one provides a subroutine which will calculate y for given values of the variables. To take into account the temperature dependence of various variables, the variables were fitted to a polynomial in temperature (see Appendix A).

6. TESTS ON INTEGRATION EFFICIENCY

6.1 Accuracy

For this test, the subroutine which calculates the value of y , did so using constant specific heats and thermal conductivities, thus enabling an analytical solution to be obtained.

The results were, at 240 cm

Analytical solution $T_2 = 3098.25$

Runge-Kutta integration

240, 1 cm steps $T_2 = 3098.25$

24, 10 cm steps $T_2 = 3098.22$

5 cm was chosen as the step size, and this resulted in temperature steps of no more than 30°, which was felt adequate to cover temperature varying properties.

6.2 Stability

This of course is very difficult to determine for all cases, however one test applied was to integrate forward over the length of the heat exchanger, and the, using the endpoint of this integration, to integrate back to the startpoint. The worst result, with 5 cm step size, was .05 degree lack of matching at the end of this second integration.

7. DESIGN OF THE DISSOCIATION HEAT EXCHANGER

The Energy Conversion prototype consisted of a two start thread machined onto the outside of a pipe, with a larger pipe shrink-fitted over this thread. This results in two channels, each .1 cm square, with a wall thickness between them of .05 cm. Actual dimensions of the pipes involved are shown in Fig. 3. The design is more fully described by Revie.[5] This prototype was designed for a mass flow rate of .5 grams per second, approximately one-tenth of the flow rate necessary for a mirror of ten square metre aperture.

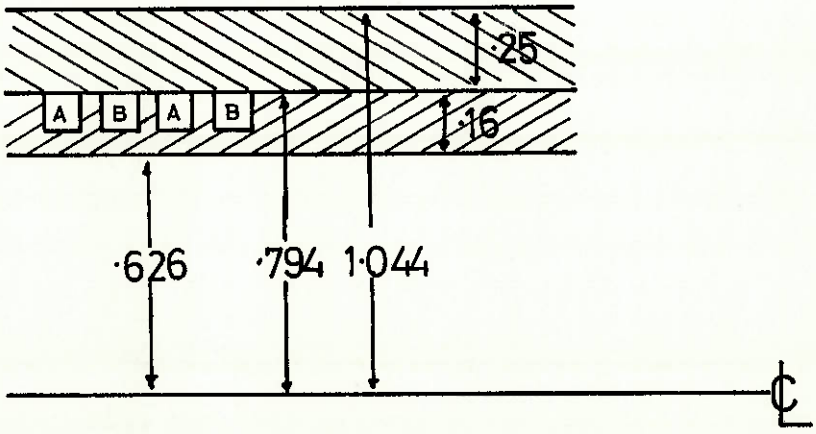

Figure 3.

8. CALCULATIONS ON THE DISSOCIATION HEAT EXCHANGER

8.1 Heat Transfer Between the Channels

The difficulty here arises due to the varying path lengths for heat transfer through the metal. If the thermal resistance of the metal were negligible compared to that of the boundary layers, this problem could be ignored, however this is not the case. Accordingly, using typical h and k values, a relaxation calculation was undertaken to determine the temperature distribution between the two channels, and this enables an estimate of the

conductivity to be made. The relaxation method is well documented in Schneider.[6] The area calculated is shown in Fig. 4. Fig. 5 shows the result of the calculation, with the orthogonal heat transfer lines as well. By defining $\bar{U}_1$ as the conductivity calculated on the basis of two walls, .2 cm wide (the length of half the perimeter of the pipes), separated by .05 cm of metal, we can see that the conductivity between the channels will be .70 $\bar{U}_1$. This factor takes into account the proximity of the inner metal boundary.

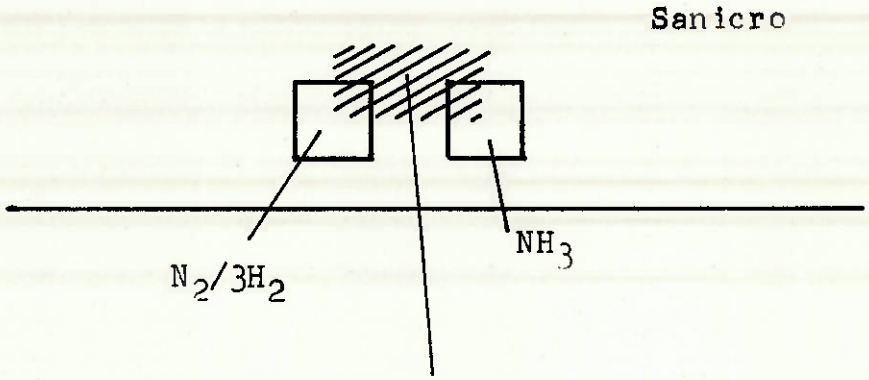

Figure 4. Calculated Area.

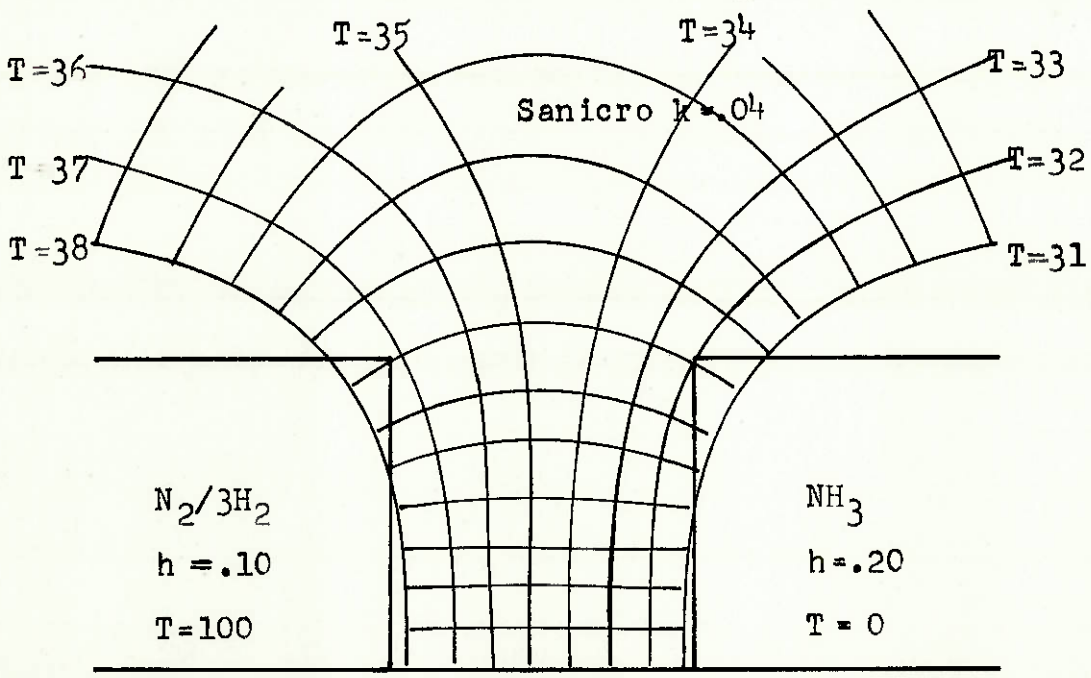

Figure 5.

8.2 Temperature Distribution Along the Heat Exchanger

Due to the heat exchanger configuration, the heat transfer between the channels is no longer simple.

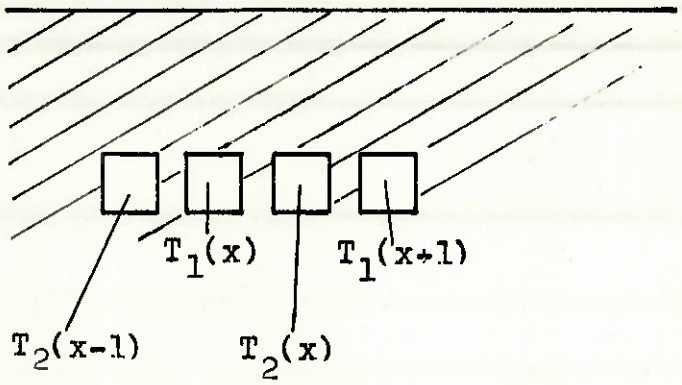

Figure 6.

Figure 6 illustrates the problem, and shows that:

$$d\dot{Q}_2 = \bar{U}_1\, dx\, (T_1(x) - T_2(x)) + \bar{U}_1\, dx\, (T_1(x+1) - T_2(x))$$

(The $\bar{U}_1$'s are assumed to be equal)

and:

$$d\dot{Q}_1 = \bar{U}_1\, dx\, (T_1(x) - T_2(x)) + \bar{U}_1\, dx\, (T_1(x) - T_2(x-1))$$

In this case l is the length of one turn of the thread (4.66 cm). To avoid the possibility of integrating a difference equation, it was assumed that

$$T_1(x+1) = T_1(x) + \frac{dT_1(x)}{dx}\, 1$$

$$T_2(x-1) = T_2(x) - \frac{dT_2(x)}{dx}\, 1$$

Hence $\frac{dT_{1,2}}{dx}$ can be obtained from:

$$\dot{m}\ c_{p1}\ \frac{dT_1}{dx} = 2\bar{U}_1\ (T_1 - T_2) + \bar{U}_1\ 1\frac{dT_2}{dx}$$

and $$\dot{m}\ c_{p2}\ \frac{dT_2}{dx} = 2\bar{U}_1\ (T_1 - T_2) + \bar{U}_1\ 1\frac{dT_1}{dx}$$

Figure 7(b) shows how the temperature of the $N_2/3H_2$ gas leaving the heat exchanger varies with the assumed total length of the heat exchanger. For these calculations, it was arranged that the $N_2/3H_2$ gas was always entering the heat exchanger at 700°C, and the NH_3 always entering at 25°C. Figure 7(a) shows the effect on the exiting NH_3 temperature. A typical temperature profile of the heat exchanger is shown in Figure 8. The length scale on the diagram is measured helically along the thread. Note that this shows heat will have to be added to the ammonia to raise it to 700°C, however it is not mandatory to add the heat at this particular (high) temperature.

9. SYNTHESIS HEAT EXCHANGER

As yet no firm design of the energy recovery system has been made. However, if the system were to be a simple ammonia synthesis plant, operating at 300 atm and 450°C, a heat exchanger would be needed to operate between ambient and this temperature. As the NH_3 synthesis does not proceed to completion, the hot side of the heat exchanger would consist of a mixture of ammonia and the gases nitrogen and hydrogen. It is expected that the molar ratio would be one part ammonia to five parts gases.

The problem here arises due to the liquefaction of ammonia near 90°C, and below this temperature, different equations need to be used.

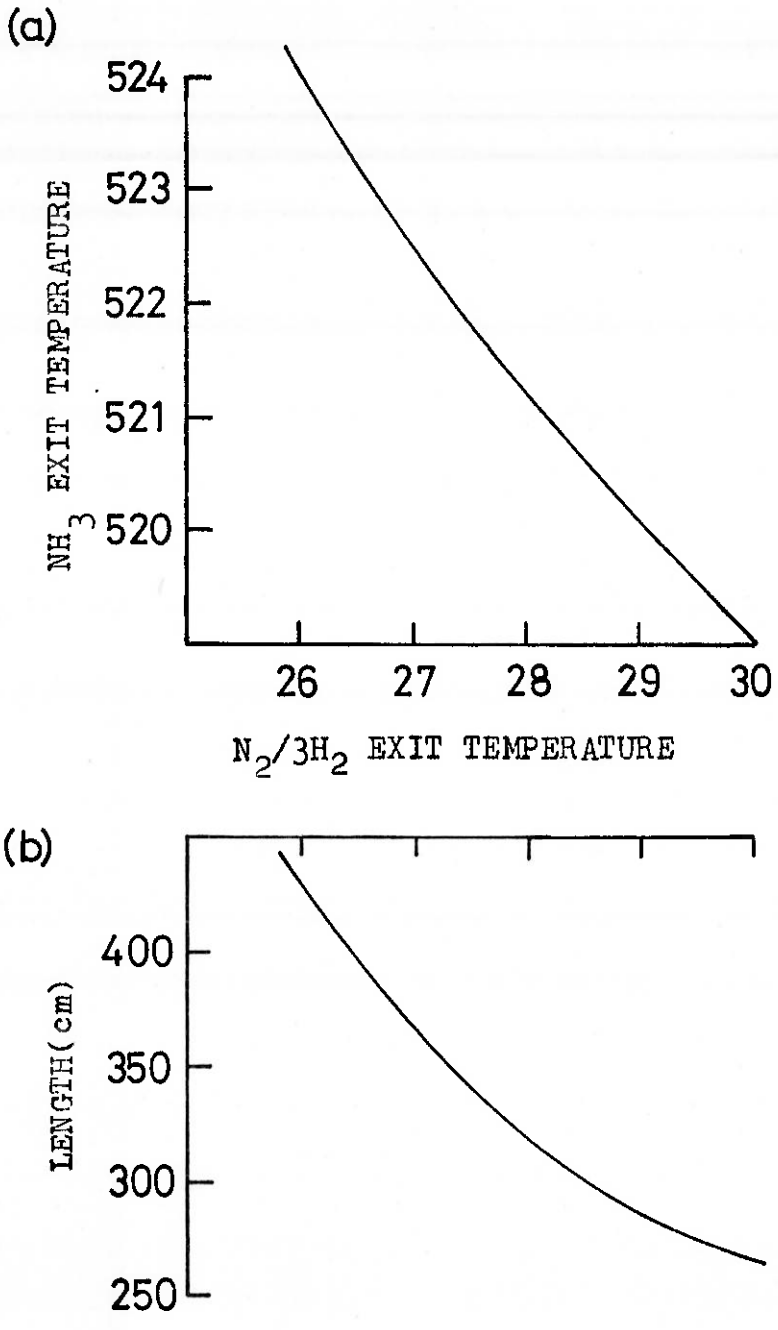
(a)
524
523
522
521
520
NH_3 EXIT TEMPERATURE
26
27
28
29
30
$N_2/3H_2$ EXIT TEMPERATURE
(b)
400
350
300
250
LENGTH(cm)

Figure 7.

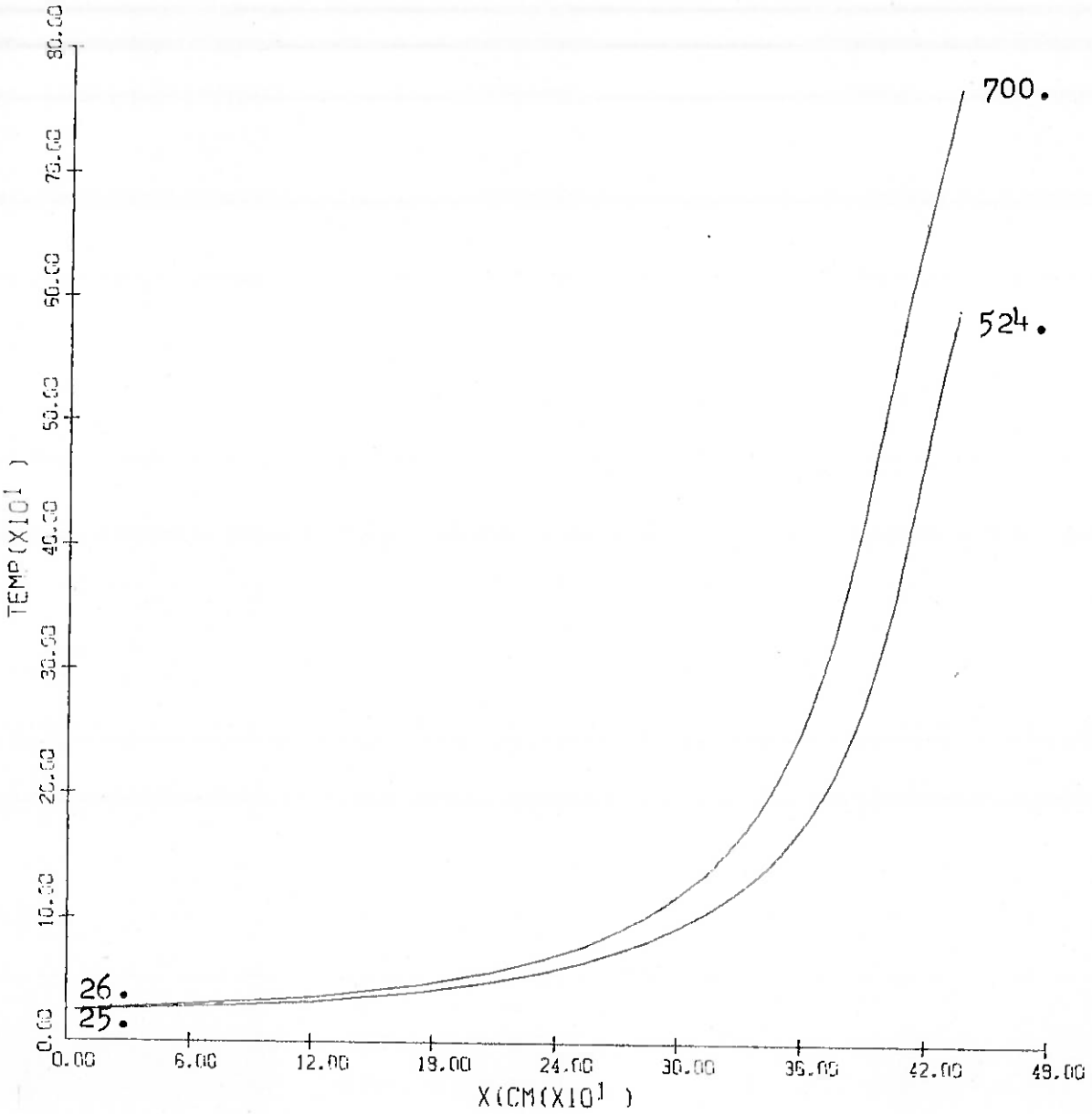
700.
524.
26.
25.
TEMP(X10¹)
X(CM(X10¹)
0.00
6.00
12.00
18.00
24.00
30.00
36.00
42.00
48.00
Distance along heat exchanger(cm)

Figure 8.

Subscripts

a - $N_2/3H_2$ gas

b - NH_3

g - gas

f - liquid

s - system

We assume that the system pressure is constant, and note that the partial pressure of the ammonia gas is determined by the vapour pressure at that temperature. We need to work out how much vapour condenses in each integration step. We assume the gases present are ideal, and thus

$$P_a V = n_a RT$$

$$P_{bg} V = n_{bg} RT$$

$$P_a n_{bg} = P_{bg} n_a$$

Now $$P_s = P_a + P_{bg}$$

$$n_{bg} = \frac{n_a P_{bg}}{P_s - P_{bg}}$$

and thus $$\Delta n_{bg} = n_a \frac{P_s}{(P_s - P_{bg})^2} \Delta P_{bg}$$

Now we approximate ΔP_{bg} by $\frac{dP_{bg}}{dT} \Delta T$, where $\frac{dP_{bg}}{dT}$ is easily obtained from vapour pressure data, and also noting that

$$\frac{n_a}{n_b} = \frac{n_a}{n_{bg} + n_{bf}} = 5$$

and that $$\frac{\Delta \dot{m}_{bg}}{\dot{m}_b} = \frac{\Delta n_{bg}}{n_b}$$

Then

$$d\dot{Q} = \left(\dot{m}_a c_{pa} + \dot{m}_{bg} c_{pbg} + \dot{m}_{bf} c_{pbf} + \frac{L(T).5.\dot{m}_b P_s}{(P_s - P_{bg})^2} \frac{dP_{bg}}{dT}\right) \Delta T$$

where L(T) is the latent heat per gram.

Thus equations similar to (1) and (2) can be developed.

In this case a straight heat exchanger was considered, which, apart from this fact, was identical in channel size, wall thickness and mass flow rate to the dissociation heat exchanger.

9.1 Properties of the Mixture

As stated before, the mixture (hot) side of the heat exchanger consists of $N_2/3H_2$ and NH_3 in a 5:1 molar ratio. Hence the viscosities were combined in this ratio, but the specific heats were combined in a 10:1 ratio, as these quantities are mass intensive. This second fact means that above 90°C both sides of the heat exchanger have near identical specific heats. Reference to eqn (3) on page 4 shows that the resulting temperature profiles will be straight. As viscosity is not a strong function of pressure, nor is heat transfer a strong function of viscosity; the viscosity of NH_3 at 300 atmospheres was used at all temperatures.

9.2 Results

In all cases the mixture entered the heat exchanger at 450°C and the $N_2/3H_2$ entered the heat exchanger at 25°C. Table 1 and Figure 9 show the basic parameters obtained from the calculations. Figure 10 shows the temperature profile and the ammonia gas partial pressure.

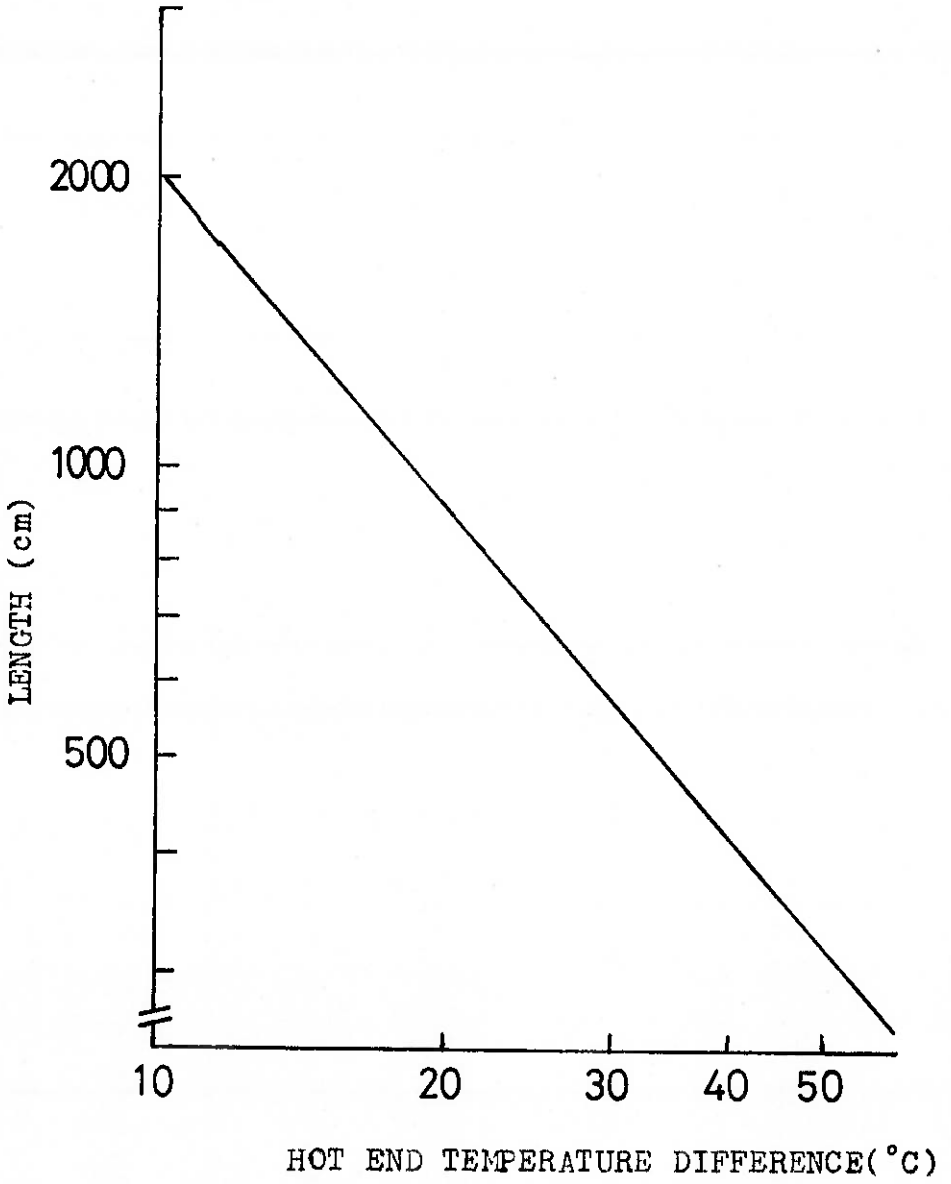
2000
1000
500
LENGTH (cm)
10
20
30
40
50
HOT END TEMPERATURE DIFFERENCE(°C)

Figure 9.

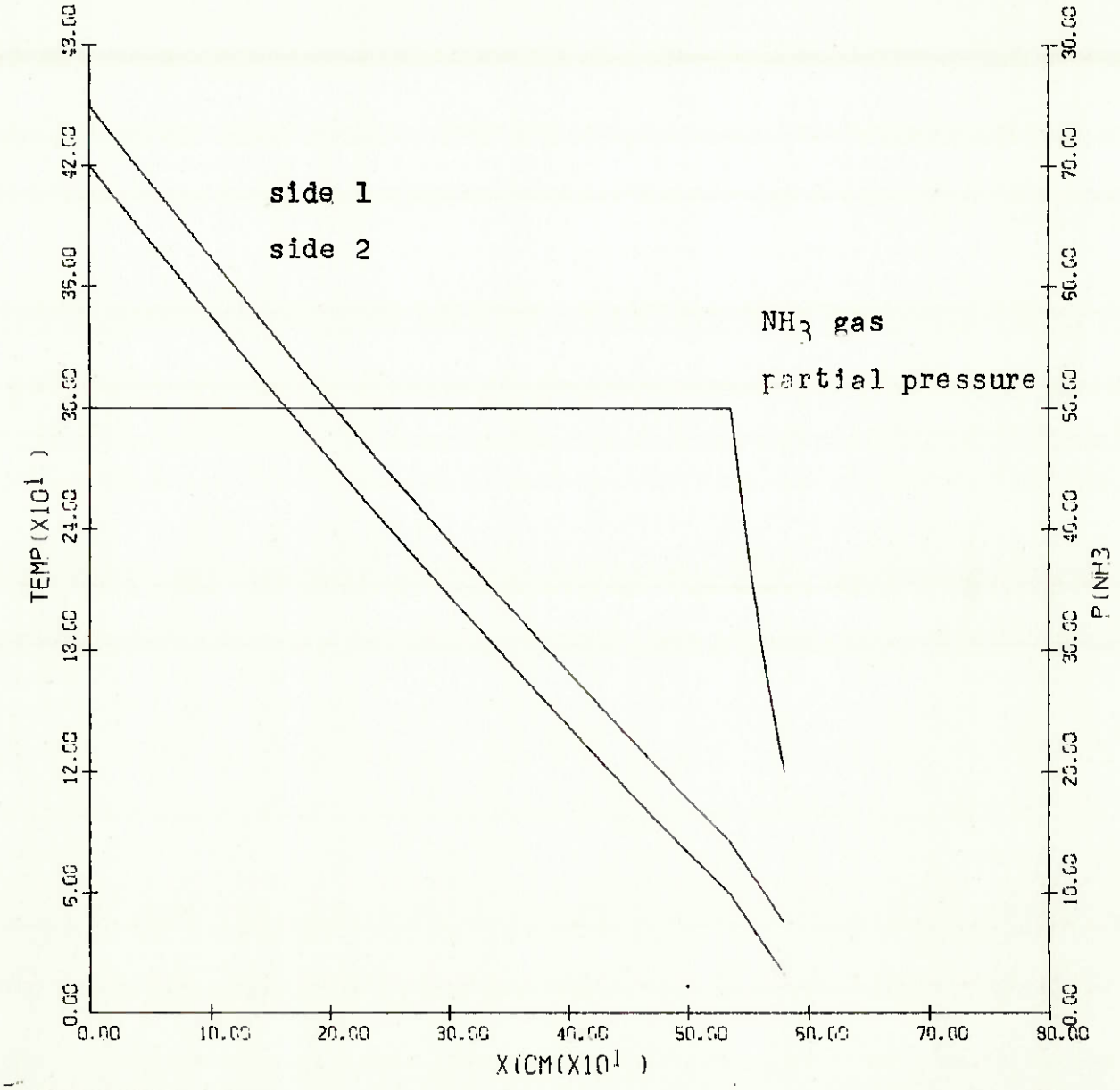
side 1
side 2
NH_3 gas
partial pressure
TEMP(X10¹)
P(NH3
X(CM(X10¹)
0.00
10.00
20.00
30.00
40.00
50.00
60.00
70.00
80.00
6.00
12.00
18.00
24.00
30.00
36.00
42.00
48.00
10.00
20.00
30.00
40.00
50.00
60.00
70.00

Figure 10.

TABLE 1

Exit Temperature $N_2/3H_2$ (^oC)	Exit Temperature Mixture (^oC)	Length (cm)
440	31.6	2091
430	41.5	907
420	51.5	573
410	61.4	417
400	71.4	323

It should be noted that this is not a simulation of the synthesis heat exchanger, as it would be a device common to all mirrors, and thus involving mass flow rates differing by three orders of magnitude from this case. It is however, clear that the difference in specific heats between the two channels is not sufficient to cause considerable deviation from a linear temperature profile. Even below 90^oC the kink in the profile is due to the increase in ammonia viscosity increasing the heat transfer, not the specific heat variation. It should be noted that as the hot end temperature difference is essentially equal to the cold end temperature difference the system constitutes a leak of energy due to having to make up the hot end temperature difference while losing the cold end energy.

10. REFERENCES

1. Carden, P. O., Energy Conversion Technical Report No. 8, Department of Engineering Physics, Australian National University.
2. Zemansky, M. W., "Heat and Thermodynamics", McGraw-Hill (1957).
3. Sandvik (Aust) Pty Ltd.
4. Gear, C. W., "Numerical Initial Value Problems in Ordinary Differential Equations".
5. Revie, R. W., Energy Conversion Technical Report No. 9.
6. Schneider, P. J., "Conduction Heat Transfer".

11. SYMBOLS

Cp	specific heat (cal/gm)
h	convection coefficient
h_l	convection coefficient per unit length
k	thermal conductivity (cal/cm/sec/^{o}C)
L	length of heat exchanger
$L(T)$	latent heat of vaporization (cal/gm)
$\dot{m}$	mass flow (gm/sec)
n	number of moles
P	pressure
$\dot{Q}$	heat flow (cal/sec)
T	temperature
$\bar{U}_e$	thermal conductivity per unit length
Λ	log mean temperature difference

APPENDIX A

CURVE FITTING AND RESULTS

The subroutine LLSQ from the IBM SSP package was used. This subroutine takes two matrices A and B and finds a matrix of coefficients X so that the Euclidean norm of (AX - B) is a minimum. Thus for polynomial fitting the i^{th} row of A is set up as $(1, T_i, T_i^2 \ldots\ldots\ldots T_i^R)$ where R is the order of the fit. The specific heat fits were found by differentiating enthalpy fits. Coefficients for the fits are shown in Table 2, the values derived from these expressions are shown in Table 3, indexed as in Table 2.

TABLE 2

```
      DIMENSION T(2),DT(2),CP(2)
      DO 1 IT=50,700,50
      T(1)=IT
      T(2)=IT
      TAV=(T(1)+T(2))/2.
C  SPECIFIC HEAT OF N2/3H2 AT 300 ATMOSPHERES...(A)
      CP(1)=.8150611-T(1)*(-4.7918E-05+T(1)*(+4.14712E-07+T(1
     /  )*(-3.676928E-10)))
C  SPECIFIC HEAT OF NH3 AT 300 ATMOSPHERES...(B)
      CP(2)=-.2233513E+00+T(2)*(2.78105E-02+T(2)*(-1.42830E-04
     1  + T(2)*(2.760122E-07+T(2)*(-2.0885E-10+T(2)*(4.154802E-14)))))
C  SPECIFIC HEAT OF NH3 GAS AT 50 ATMOSPHERES...(C)
      CPBG=.7337952-T(2)*5.485768E-05
C  SPECIFIC HEAT OF NH3 LIQUID AT 50 ATMOSPHERES...(C)
      IF(IT.LT.90)CPBG=.882785+T(1)*6.08113E-03
C  THERMAL CONDUCTIVITY OF THE SANICRO ALLOY...(D)
      ASNCRO=(((.12036E-12*TAV-.884095E-10)*TAV-.152403
     1  E-07)*TAV+.527749E-04)*TAV+.0259513
C  VISCOSITY OF N2/3H2 AT 300 ATMOSPHERES...(E)
      ATN2H2=.104214E-03+T(1)*(.257464E-06-T(1)*0.815083E-10)
C  VISCOSITY OF NH3 AT 300 ATMOSPHERES, TEMPERATURE LESS THAN 104 C
      ATANH3=0.201483E-02-T(2)*0.157287E-04
C  GREATER THAN 104 DEGREES C...(G)
      IF(T(2).GT.104.)ATANH3=0.432501E-03+T(2)*(-0.503691E-06
     1  +T(2)*0.615696E-09)
    1 WRITE(3,300)T(1),CP(1),CP(2),CPBG,ASNCRO,ATN2H2,ATANH3
  300 FORMAT(1X,F7.1,6(2X,1PE9.2))
      END
```

TABLE 3

	(A)	(B)	(C)	(D)	(E)	(G)
50.0	8.16E-01	8.43E-01	1.19E+00	2.85E-02	1.17E-04	1.23E-03
100.0	8.16E-01	1.38E+00	7.28E-01	3.10E-02	1.29E-04	4.42E-04
150.0	8.14E-01	1.56E+00	7.26E-01	3.33E-02	1.41E-04	3.71E-04
200.0	8.11E-01	1.51E+00	7.23E-01	3.54E-02	1.52E-04	3.56E-04
250.0	8.07E-01	1.34E+00	7.20E-01	3.73E-02	1.63E-04	3.45E-04
300.0	8.02E-01	1.13E+00	7.17E-01	3.90E-02	1.74E-04	3.37E-04
350.0	7.97E-01	9.32E-01	7.15E-01	4.06E-02	1.84E-04	3.32E-04
400.0	7.91E-01	7.92E-01	7.12E-01	4.20E-02	1.94E-04	3.30E-04
450.0	7.86E-01	7.22E-01	7.09E-01	4.35E-02	2.04E-04	3.31E-04
500.0	7.81E-01	7.21E-01	7.06E-01	4.50E-02	2.13E-04	3.35E-04
550.0	7.77E-01	7.68E-01	7.04E-01	4.67E-02	2.21E-04	3.42E-04
600.0	7.74E-01	8.27E-01	7.01E-01	4.86E-02	2.29E-04	3.52E-04
650.0	7.72E-01	8.47E-01	6.98E-01	5.10E-02	2.37E-04	3.65E-04
700.0	7.72E-01	7.68E-01	6.95E-01	5.40E-02	2.44E-04	3.82E-04